BIOCHEMISTRY
including biophysical chemistry & molecular biology
Article

Biochemistry **2009,** *48,* 10549–10557 10549
DOI: 10.1021/bi901261y

Sortase Activity Is Controlled by a Flexible Lid in the Pilus Biogenesis Mechanism of Gram-Positive Pathogens[†,‡]

Clothilde Manzano, Thierry Izoré, Viviana Job, Anne Marie Di Guilmi, and Andréa Dessen*

Institut de Biologie Structurale Jean-Pierre Ebel, UMR 5075 (CEA, CNRS, UJF), 41 rue Jules Horowitz, F-38027 Grenoble, France

Received July 23, 2009; Revised Manuscript Received October 7, 2009

ABSTRACT: Pili are surface-linked virulence factors that play key roles in infection establishment in a variety of pathogenic species. In Gram-positive pathogens, pilus formation requires the action of sortases, dedicated transpeptidases that covalently associate pilus building blocks. In *Streptococcus pneumoniae*, a major human pathogen, all genes required for pilus formation are harbored in a single pathogenicity islet which encodes three structural proteins (RrgA, RrgB, RrgC) and three sortases (SrtC-1, SrtC-2, SrtC-3). RrgB forms the backbone of the streptococcal pilus, to which minor pilins RrgA and RrgC are covalently associated. SrtC-1 is the main sortase involved in polymerization of the RrgB fiber and displays a lid which encapsulates the active site, a feature present in all pilus-related sortases. In this work, we show that catalysis by SrtC-1 proceeds through a catalytic triad constituted of His, Arg, and Cys and that lid instability affects protein fold and catalysis. In addition, we show by thermal shift analysis that lid flexibility can be stabilized by the addition of substrate-like peptides, a feature shared by other periplasmic transpeptidases. We also report the characterization of a trapped acyl-enzyme intermediate formed between SrtC-1 and RrgB. The presence of lid-encapsulated sortases in the pilus biogenesis systems in many Gram-positive pathogens points to a common mechanism of substrate recognition and catalysis that should be taken into consideration in the development of sortase inhibitors.

Pili are extracellular flexible fibers that are directly associated to the bacterial cell wall and play key roles in initiation of bacterial infection. These important virulence factors are essential for adhesion to target host cells, motility, and DNA transformation and have been shown to considerably enhance bacterial ability to attach to host tissue and initiate colonization (*1*, *2*). In contrast to pili located on the surface of Gram-negative bacteria, which are formed by the noncovalent association of subunits (*3*, *4*), Gram-positive pili have been shown to be formed by covalently associated building blocks. Pathogens such as *Corynebacterium diphtheriae*, *Streptococcus pyogenes*, and *Streptococcus pneumoniae* carry all of the genes required for generation of the entire pilus-forming machinery within a single pathogenicity islet (*5*−*8*). Thirty percent of pathogenic strains of *S. pneumoniae*, the causative agent of pneumonia, septicemia, and meningitis, carry the *rlrA* pathogenicity region, which codes for a transcriptional regulator (RlrA), three structural proteins (RrgA, RrgB, and RrgC), and three sortases (SrtC-1, SrtC-2, and SrtC-3). Electron microscopy and genetic studies of infectious pneumococcal strains have shown the pilus backbone fiber to be formed by RrgB subunits, while RrgA and RrgC are minor pilins that are directly associated to the polymerized RrgB fiber (*5*, *8*, *9*). Both RrgA and RrgC play important roles in infectivity and target cell recognition (*9*, *10*), while SrtC-1, SrtC-2, and SrtC-3 catalyze the intramolecular association of Rrg molecules (*11*−*14*).

Sortases are cysteine transpeptidases that participate in a variety of processes, including surface attachment of virulence factors, sporulation, and iron acquisition (*15*, *16*). SrtA and SrtB from *Staphylococcus aureus* represent the best-studied sortases to date. These enzymes recognize an LPXTG-like motif within the sequence of secreted virulence factors, catalyze the nucleophilic attack of the Thr−Gly bond, and finally associate the target proteins carrying the LPXT- sequence directly to the peptidoglycan stem peptide (*17*−*19*). The structures of SrtA and SrtB reveal a β-barrel fold displaying a triad of catalytic residues (Cys, His, Arg) on exposed extremities of three adjacent strands (*20*, *21*); the identification of Cys as the catalytic residue responsible for nucleophilic attack was shown not only by mutagenesis studies, in which introduction of an Ala at this site abolishes catalysis, but also by crystallization of covalent complexes between sortases and ligands which are covalently associated to the Cys residue (*22*−*24*). In addition, the structure of SrtA in complex with an LPXTG-like peptidyl-sulfhydryl compound reveals a covalent interaction between the peptide and the catalytic Cys (*25*). Notably, while mutagenesis of His or Arg side chains dramatically affects catalytic efficiency in SrtA, the precise role played by these residues is still a matter of controversy (*18*, *26*−*28*).

Within the pneumococcal pilus system, RrgA, RrgB, and RrgC all carry LPXTG-like motifs on their C-termini, suggesting that these regions are targeted by sortases (*5*, *29*, *30*). Although the equal number of structural and sortase-encoding genes in pneumococci originally implied that each sortase could be exclusively dedicated to one Rrg molecule (*5*), recent work has shown that pilus sortases have interchangeable specificities to a certain extent (*11*, *31*). Nevertheless, SrtC-1 was shown to be the main

[†]This work was supported by EC Grant LSHM-CT-2004-512138 (to A.D.).

[‡]The coordinates of SrtC-1 H131D were deposited in the Protein Data Bank with code 2WTS and are available prerelease from the authors.

*To whom correspondence should be addressed: e-mail, andrea.dessen@ibs.fr; phone, (33)4-38-78-95-90; fax, (33)4-38-78-54-94.

Published on Web 10/07/2009

sortase involved in polymerization of the RrgB fiber (*31*) while the other two sortases also recognize the coadjuvant adhesin molecules (*5*, *11*, *12*). The recent structures of the three pilus-related sortases (SrtC-1, SrtC-2 SrtC-3 from *S. pneumoniae*) revealed that these enzymes, like their nonpilus-associated counterparts, also fold into β-barrels and carry Cys, His, and Arg side chains within the active site cleft (*14*, *31*). Cys193 was shown to be essential for RrgB fiber formation by SrtC-1; the wild-type enzyme could generate elongated RrgB fibers *in vitro*, while a Cys193Ala mutant showed no activity (*31*). Additionally, a noteworthy feature of the pilus-related sortases involves the presence of a lid that not only blocks active site access but also carries two key residues, which are invariably an Asp and a hydrophobic amino acid, that make interactions within the catalytic cleft itself, serving as "anchors". Although sequences corresponding to lid regions can be identified in all pilus-related sortases characterized to date (*31*), the function of this feature, as well as the roles played by the two other residues in catalysis, has remained obscure.

In this work, we investigate the functions of both the lid and catalytic triad regions in the pilus fiber-formation activity of SrtC-1. We employ thermal shift assay (TSA)[1] techniques to show that the lid region of SrtC-1 plays roles both in stabilizing the enzyme and in allowing substrate access to the active site. In addition, we show that amino acids His131 and Arg202 are essential for RrgB fiber formation and that Arg202, in particular, also plays a structural stabilization role through interaction with lid anchors. Lastly, we describe the "trapping" of a covalent complex between RrgB and SrtC-1, which can be observed by SDS−PAGE and LC-MS/MS spectrometry analysis. The absolute requirement for sortases in the pilus-formation processes of all Gram-positive pathogens, coupled to the presence of lid regions with similar anchor residues in these enzymes, suggests that these data will contribute to the understanding of the pilus-formation mechanism in a variety of infectious organisms.

MATERIALS AND METHODS

Generation of Mutants SrtC-1 H131D, SrtC-1 R202E, SrtC-1 D58G/W60G, and SrtC-1 C193A/D58G/W60G. The expression plasmid pLIMSrtC-1 encoding wild-type His_6-SrtC-1 (or His_6-SrtC-1 C193A) served as a template for the introduction of single amino acid substitutions by PCR using the QuickChange II site-directed mutagenesis kit (Stratagene). All mutant constructs were subsequently sequenced; the results showed that only expected mutations were introduced during PCR.

Expression and Purification of Recombinant Proteins. Protein expression in *Escherichia coli* BL21(DE3)-RIL was similar in all cases and was induced in Terrific broth with 1 mM IPTG at 37 °C for 3 h. Cells were harvested by centrifugation and lysed by sonication in buffer A (50 mM Tris-HCl, pH 8.0, 0.2 M NaCl, 20 mM imidazole). Supernatants were cleared by centrifugation and applied to a HisTrap column (GE Healthcare), preequilibrated in buffer A. Proteins were eluted with a imidazole gradient and were subsequently cleaved by Tev protease overnight at 4 °C. Recombinant proteins were then submitted to further purification on a gel filtration column in 50 mM HEPES, pH 7.0, and 0.15 M NaCl. All mutant proteins were verified by mass spectrometry analysis.

[1]Abbreviations: TSA, thermal shift assay; LC-MS, liquid chromatography/mass spectrometry.

In Vitro RrgB Fiber Formation. Recombinant purified RrgB was incubated with SrtC-1, SrtC-1 H131D, or SrtC-1 R202E at a 1:4 (w/w) ratio in a total volume of 15 μL and subsequently incubated overnight at 37 °C. Each aliquot was mixed with XT sample buffer and XT reducing agent (Bio-Rad), boiled for 10 min, and loaded onto 4−12% Criterion XT precast gels (Bio-Rad). Gels were subsequently electrotransferred into Trans-Blot transfer medium (Bio-Rad). Membranes were blocked with 5% nonfat milk in PBS with 0.3% Tween (PBS-T) for 1 h at room temperature. Membranes were left in primary antiserum (anti-RrgB or anti-SrtC-1 polyclonal mouse antibodies diluted to 1:5000) during 1.5 h at room temperature. After three successive 10 min washes in PBS-T, the membranes were incubated with secondary anti-mouse HRP-conjugate antibodies (Sigma, diluted 1:10000) overnight at 4 °C. Detection of HRP activity was performed directly on the membranes with SIGMA-FAST DAB tablets (Sigma).

Lid Replacement Mutagenesis. The construction of a mutant form of SrtC-1 carrying the lid region of SrtC-2 (residues 52−78), as well of SrtC-2 carrying the lid region of SrtC-1 (residues 43−69), was performed by using the restriction-free cloning technique, based on two PCR steps. In the first PCR step the desired lid was amplified using two primers (50−55 bases long), with a 25−28 base overlap within the desired point of insertion and 26−29 bases complementary to the vector. A second PCR was subsequently performed using as a template the vector of interest and as a primer the purified product of the first PCR step. At the end of the reactions the methylated parental plasmids were digested with *Dpn*I for 3 h at 37 °C. All PCR reactions were performed using 1 unit of *Pfu* DNA polymerase (Fermentas) in a 50 μL reaction. The final products were used to transform *E. coli* NEB5α-competent cells, and the lid substitutions were verified by DNA sequencing.

Fluorescence-Based Protein Thermal Stability Assays. Assays were conducted in an IQ5 96-well format real-time PCR instrument (Bio-Rad) in the presence of a Sypro Orange (Molecular Probes) probe. The total volume was 25 μL. Samples were heat-denatured from 20 to 100 °C at a rate of 1 °C per minute for SrtC-1 H131D and SrtC-1 R202E mutants and from 20 to 80 °C at a rate of 0.5 °C per minute for SrtC-1 D58G/W60G and SrtC-1 C193A/D58G/W60G mutants. At each step, excitation was performed at 470 nm, while emission of Sypro Orange fluorescence was monitored at 570 nm. Plotting of the fluorescence vs temperature curves, followed by the calculation of the first derivative at each point, allowed the identification of each inflection point; the minima were referred to as the melting temperatures (T_m). The SrtC-1 C193A/D58G/W60G variant was employed for experiments with the IPQTG and YPRTG peptides (PSL GmbH), in order to avoid the potential catalytic reaction of the substrates with the active site Cys193. Prior to experimentation with peptides, SrtC-1 C193A/D58G/W60G and SrtC-1 D58G/W60G variants were shown to display identical purification profiles and TSA T_m values (not shown). Peptides were added to the experiment in a final molar ratio of 1:10 and 1:20 (protein:peptide). Each result is representative of three independent experiments.

Crystallization, Data Collection, and Structure Solution. SrtC-1 H131D crystals crystals were obtained in hanging drops in 0.1 M Tris, pH 8.5, 0.2 M $MgCl_2$ hexahydrate, and 30% PEG4000 at room temperature and were cryoprotected by gradual incubation in increasing amounts of glycerol to a final concentration of 20%. Diffraction data were collected at the

Table 1

	SrtC-1 H131D
Data Collection	
X-ray source	ID29
detector	ADSC Q315
space group	$P2_12_12_1$
unit cell parameters (Å)	$a = 68.4$, $b = 70.5$, $c = 87.3$
wavelength (Å)	0.98088
resolution (Å)	3.9−1.3 (1.4−1.3)
no. of unique reflections	99255 (14789)
completeness (%)	95.3 (88.9)
mosaicity (deg)	0.16
R_{sym}	5.4 (36.4)
$I/\sigma(I)$	17.0 (4.2)
Refinement	
resolution (Å)	19.8−1.3
R_{work} (%)	15.7
R_{free} (%)	19.5
no. of protein atoms	3286
no. of solvent atoms	670
no. of glycerol molecules	3
rms deviation, bond lengths (Å)	0.01
rms deviation, bond angles (deg)	1.41
mean B-factor (Å^2)	14.9
Ramachandran favored (%)	98.7

European Synchrotron Radiation Facility (ESRF) beamline ID29 (Grenoble, France). Diffraction images were indexed and scaled with XDS (*32*). The structure was solved by molecular replacement using the program PHASER (*33*) employing the structure of wild-type SrtC-1 as a search model. Model building and refinement steps were performed with Coot and REFMAC 5.4 (*34*, *35*). Data collection and structural refinement statistics are shown in Table 1. Figures were generated with PyMOL (http://www.pymol.org).

Mass Spectrometry Analysis. The band identified in Figure 4A with a star was excised from the gel and subsequently washed with 50 mM acetonitrile/ammonium bicarbonate, 50/50 (v/v), for 30 min before dehydratation with acetonitrile. Subsequently, the sample was treated with 7% H_2O_2. After drying was complete, the band was rehydrated in 15 μL of digestion buffer (50 mM ammonium bicarbonate, pH 8.1) containing 150 ng of trypsin and incubated at 4 °C for 15 min. Digestion buffer (30 μL) was then added, and the digestion reaction was carried out at 37 °C overnight. Peptides were extracted from the gel by diffusion for 15 min with agitation, followed by three sequential 5 min sonication steps in 50% acetonitrile, 5% formic acid, and 100% acetonitrile. Digestion and extraction solutions were pooled and dried under vacuum. Peptide mixtures were redissolved in 25 μL of water/acetonitrile 95/5 (v/v) containing 0.2% trifluoroacetic acid prior to LC-MS/MS analysis. All experiments were performed in a 96-well system coordinated by an EVO15 (Tecan) robot (EdyP, Grenoble).

RESULTS

RrgB Fiber Formation Requires a Catalytic Triad. SrtC-1 is the main sortase involved in formation of the RrgB pilus fiber, and mutation of its catalytic cysteine (Cys193) into Ala abolishes fiber-forming activity (*11*, *31*). The high-resolution structure of SrtC-1 from infectious pneumococcal strain TIGR4 revealed

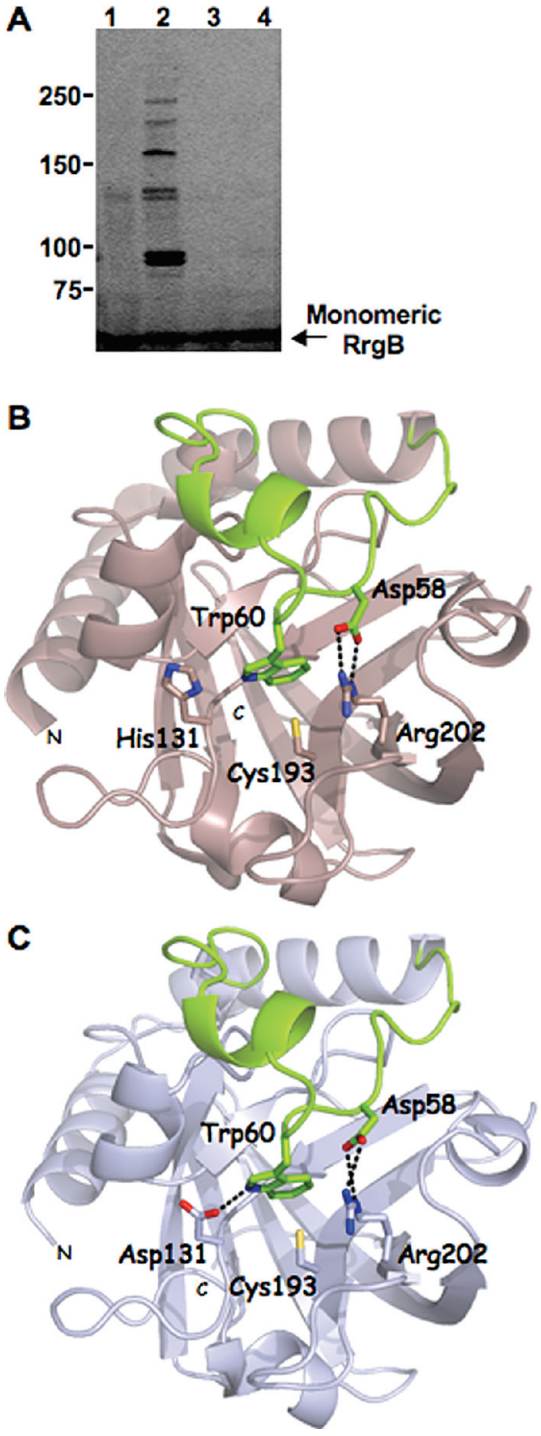

FIGURE 1: The active site of SrtC-1 contains a catalytic triad. (A) Western blot developed with RrgB antiserum. Lanes: (1) monomeric RrgB; (2) RrgB + SrtC-1; (3) RrgB + SrtC-1 H131D; (4) RrgB + SrtC-1 R202E. Molecular mass standards (in kDa) are indicated on the left. (B) Active site of wild-type SrtC-1 and (C) active site of SrtC-1 H131D. The active site residues are shown as sticks, and the lid region is colored green.

that, in addition to Cys193, the catalytic site also harbors His131 and Arg202; although the functions of the two latter residues were unknown, their three-dimensional arrangement is comparable to what is observed in active sites of nonpilus-related sortases, which also carry Cys, His, and Arg residues (*20*, *23*, *25*, *31*). In order to explore the functions of His131 and Arg202 in SrtC-1's fiber-forming activity, we mutated these residues into Asp and Glu, respectively, and searched for the capacity of SrtC-1

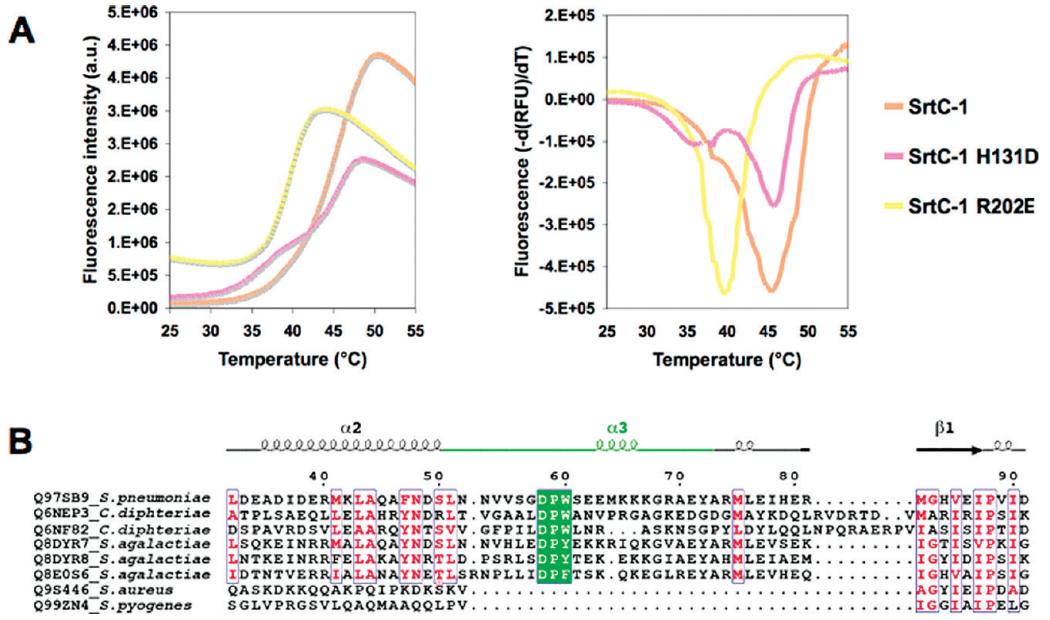

FIGURE 2: Thermal stability of active site SrtC-1 variants. (A) Thermal unfolding of SrtC-1 and two active site mutants was followed in the presence of the Sypro Orange fluorescent probe (left). The minimum of the first derivative of the thermal denaturation curve determines the inflection point, which corresponds to the melting temperature (T_m, right). (B) Sequence alignment of the lid regions of sortases involved in pilus formation in different Gram-positive pathogens (six first lines) and association of virulence factors to the peptidoglycan (two last lines). Those involved in pilus biosynthesis harbor the Asp-Pro-Hyd motif, in which the Asp and the hydrophobic residue serve as anchors within the catalytic cleft.

H131D and SrtC-1 R202E variants to generate a pattern of high molecular mass bands on SDS−PAGE upon incubation with RrgB at 37 °C (as described in ref *31*). The Western blot on Figure 1A, which was developed with anti-RrgB antibodies, confirms that wild-type SrtC-1 is able to catalyze the formation of a pattern of high molecular mass RrgB bands (which correspond to the pilus backbone fibers as shown by microscopy by Manzano and co-workers (*31*); lane 2). In contrast, neither SrtC-1 H131D (lane 3) nor SrtC-1 R202E (lane 4) was able to catalyze fiber formation. These results suggest that, as in the case of nonpilus-related sortases, SrtC-1 employs a catalytic triad composed of Cys193, His131, and Arg202 for RrgB fiber generation.

In order to address the issue of active site stability within SrtC-1 mutant structures, we submitted both proteins to crystallization trials. SrtC-1 R202E crystals were of poor quality and diffracted X-rays only to low resolution (8 Å). However, SrtC-1 H131D crystals diffracted X-rays to high resolution (1.3 Å) at the ESRF synchrotron in Grenoble, and we were able to solve its structure by employing wild-type SrtC-1 (PDB code 2WIJ) as a search model in a molecular replacement experiment (see Materials and Methods). Data collection and refinement statistics are shown in Table 1. SrtC-1 H131D displays a highly similar fold to wild-type SrtC-1 (rms deviation of 0.2 Å over 196 Cα atoms), revealing that the mutation in the catalytic cleft does not affect the general fold of the protein. Analysis of the SrtC-1 H131D active site (Figure 1C, where lid residues are shown in green) reveals only slight differences from the wild-type SrtC-1 molecule (Figure 1B). The side chain of Cys193 is present in two conformations, as is the case for wild-type SrtC-1 (only one is shown for clarity). In addition, the side chain of the mutant residue, Asp131, stabilizes the Nε group of Trp60, a lid anchor residue, through a close hydrogen bond (2.7 Å); in the wild-type structure, His131 does not make any interactions within the active site and is located 5.3 Å away from the nucleophilic cysteine. Thus, although the mutation of His131 into Asp does not affect the overall fold of the protein, Asp131 is not able to replace the catalytic function of His131, suggesting that the positive charge on His131 is crucial for SrtC-1's fiber-forming activity.

We further investigated the stability of wild-type and mutant SrtC-1 forms through thermal shift assays. Proteins were gradually heated in an IQ5 real time PCR apparatus, and thermal unfolding curves were monitored through the detection of changes in fluorescence of a Sypro Orange probe. For data analysis, the melting temperature (T_m) for each sample was determined as the minimum peak in the first derivative plot of the melting curve representing the raw fluorescence data. Results are shown in Figure 2A. This analysis reveals that the T_m values for both wild-type SrtC-1 and SrtC-1 H131D are in the range of 46 °C, while that of the SrtC-1 R202E mutant is of 39 °C. This suggests that mutation of Arg202 engenders structural destabilization of SrtC-1, which could explain the lack of success in obtaining well-diffracting crystals of this mutant. It is of note that, in the active site of the wild-type SrtC-1 molecule, lid anchor residue Asp58 interacts directly with both NH2 and Nε atoms of Arg202 (Figure 1B). The results with the SrtC-1 R202E mutant thus suggest that, at least in the absence of substrate, the Asp58−Arg202 interaction is essential for lid and overall protein stability. Thus, the lack of fiber-forming activity of SrtC-1 R202E could be linked not only to the absence of the Arg side chain for catalytic function (discussed below) but also to a decrease in structural stability.

The Sortase Lid Is Key for Activity and Stability. In all pilus-related sortases sequenced to date, lid anchor residues invariably include an Asp at a position which is homologous to that occupied by Asp58 in SrtC-1 and a large hydrophobic side chain (Trp, Tyr, or Phe) at the site occupied by Trp60 (Figure 2B). The structure of SrtC-1 shows that lid anchor residues not only interact directly with active site residues, as seen above, but the lid itself blocks an elongated cleft which could be the LPXTG substrate binding site (*31*). This hypothesis was

put forth through comparison of the structures of SrtC-1/SrtC-3 and staphylococcal SrtA, which binds an LPXTG peptidic substrate in a comparable cleft that harbors the active site residues on one end (*24*, *31*), and has also been suggested by the recent structure of SrtA in complex with a covalent substrate analogue (*25*). This could imply that one of the functions of the lid is to regulate substrate access into the cleft. In order to investigate this potential function of the lid, we constructed a SrtC-1 double mutant in which lid anchor residues Asp58 and Trp60 were mutated into glycines. Initially, we tested the ability of SrtC-1 D58G/W60G to generate a RrgB high molecular mass ladder on SDS−PAGE. As shown in the Western blot on Figure 3A, in which the same amount of sample mixture was loaded in all lanes, SrtC-1 D58G/W60G (lane 2) can recognize RrgB and generate an initial set of bands, but polymerization is less efficient than for wild-type SrtC-1 (lane 3).

To explore the effects of the two anchor side chains on the stability of SrtC-1, we performed thermal shift assay (TSA) experiments on SrtC-1 D58G/W60G. The results, shown in Figure 3B, indicate that SrtC-1 D58G/W60G displays a T_m which is 8 °C lower than that of the wild-type enzyme (38 versus 46 °C). Thus, the side chains of lid anchor residues Asp58 and Trp60 are required for SrtC-1 stability. It is of note that the SrtC-1 R202E mutant is also considerably less stable than wild-type SrtC-1 (Figure 2). This indicates that the Arg202−Asp58 interaction plays an important role in SrtC-1 stabilization and suggests that mutants that cannot generate this interaction have a lid region that tends to be in an "open" or flexible state. If so, these mutant forms could potentially be stabilized by the addition of substrate into the active site region.

In order to test this possibility, we employed the TSA technology to test if SrtC-1 D58G/W60G could be stabilized by a peptide corresponding to the RrgB LPXTG-like sequence (IPQTG). Addition of increasing amounts of peptide were accompanied by an increase in the T_m of the mutant protein (Figure 3B), suggesting that the five-residue substrate peptide can penetrate the active site of the "open lid" SrtC-1 form and stabilize its structure. These data thus strongly point to a double role for the lid region in pilus-related sortases: (1) covering of the active site in the absence of substrate and ensuring protein stability; (2) maintenance of Arg202 optimally pointed toward the active site cysteine (through the Asp58−Arg202 interaction), enabling it to efficiently participate in catalysis. The presence of a Phe and Asp residues as anchor points in the lid region of SrtC-3 (*31*), also expressed in the *rlrA* operon, suggests that lids in pilus-related sortases could play similar roles.

Recently, Fälker and co-workers (*11*) showed that SrtC-1 (named SrtB in their report), in addition to acting as a pilus polymerase, could also recognize minor pilins. We thus set out to verify this point by incubating SrtC-1 D58G/W60G with increasing amounts of YPRTG, the LPXTG-like peptide from RrgA, a minor pilin, and performing analysis through TSA, as described for the IPQTG peptide. Results show that, much as in the case of IPQTG, SrtC-1 D58G/W60G can also recognize and be stabilized by increasing amounts of YPRTG (Figure 3C). The T_m is thus shifted from 38 °C (mutant enzyme with no peptide) to 43 °C (highest amount of peptide), indicating that the peptide from a minor pilin is as successful as IPQTG in rendering SrtC-1 D58G/W60G more stable. Thus, the presence of proline, threonine, and glycine within the LPXTG-like sequence plays a key role in recognition of the motif within the sortase active site. Interestingly, Suree and co-workers (*25*) have recently proposed that the lid anchor residues in pilus-related sortases (Asp58 and Trp60 in SrtC-1) could mimic the PX portion of the peptide motif and thus occlude the LPXTG binding site. Our results are in agreement with this proposition, since the mutant that lacks both anchor residues can recognize/be stabilized by two slightly different LPXTG-like sequences. These data also suggest that pilus-related sortases do not show strict specificity for one specific LPXTG-like sequence, as proposed before (*11*, *31*).

Preferences for the individual Rrg substrates could potentially be dictated by other factors. *In vivo*, the relative abundance of unpolymerized pilins in the immediate environment of the pilus-forming machinery could play an important role. In addition, considering the structure of the sortase itself, the region of the cleft which recognizes the donor substrate (*25*) as well as the section of the lid region that faces the outside of the molecule (and not the active site) (*31*) could also be important for Rrg selection. In order to explore this latter point, we generated mutant forms of SrtC-1 and SrtC-2 in which the respective lid regions (*31*) were exchanged. Both mutant proteins (SrtC-1 (lidC-2) and SrtC-2 (lidC-1)) were tested for RrgB-polymerizing capabilities (Figure 3A, lanes 4 and 5) as well as structural stability by TSA. In both cases, the capacity to form RrgB fibers was abolished, although SrtC-1 (lidC-2) still displayed a very minor activity toward the RrgB substrate as seen by the presence of a minor band below the 100 kDa marker in Figure 3A (lane 4). Interestingly, TSA analyses of the two mutant proteins revealed results that were difficult to reproduce, indicating inherent protein instability (and are thus not shown). In addition to the lid sequences being quite distinct, SrtC-1 carries a Trp residue at position 60, while SrtC-2 carries a Phe at the analogous position; it is conceivable that the exchange of these two key anchor residues could provide an important destabilization factor in both cases. Thus, this indicates that the lid region not only provides structural stability to the sortase itself but also provides an interaction platform for recognition and selection of the Rrg substrate.

Formation in Vitro of a Covalent Complex between SrtC-1 and RrgB. Upon incubation of SrtC-1 and RrgB and analysis on SDS−PAGE, in addition to the RrgB ladder identified with anti-RrgB antibodies (Figure 1, lane 2), development of the gel with an antibody raised against SrtC-1 revealed three bands (Figure 4A, lane 2). The most prominent one represents the sortase monomer, while an intermediary band, identifiable in both the presence or absence of RrgB, represents a minor form of a sortase dimer. The other additional band migrates above the 85 kDa marker and is indicated with star in Figure 4A; interestingly, a band migrating at approximately the same point can also be identified in a gel developed with anti-RrgB serum (Figure 1 and ref *31*), indicating that it could represent a complex between RrgB and SrtC-1. In order to investigate the nature of this band, we submitted the entire mix to mass spectrometry, and the results are shown in Figure 4B. In addition to the expected masses of SrtC-1 and RrgB, we identified a form whose molecular mass (approximately 88.3 kDa) could correspond to that of a covalent complex between SrtC-1 and RrgB. In order to confirm this finding, we cleaved the band from the gel, trypsinized the sample, and performed liquid chromatography coupled to tandem mass spectrometry (LC-MS/MS). The peptides that correspond to this experiment are shown in Figure 4C, and all correspond to either RrgB or SrtC-1, indicating that this additional band corresponds to a covalent complex between RrgB and SrtC-1. Notably, the same band could be

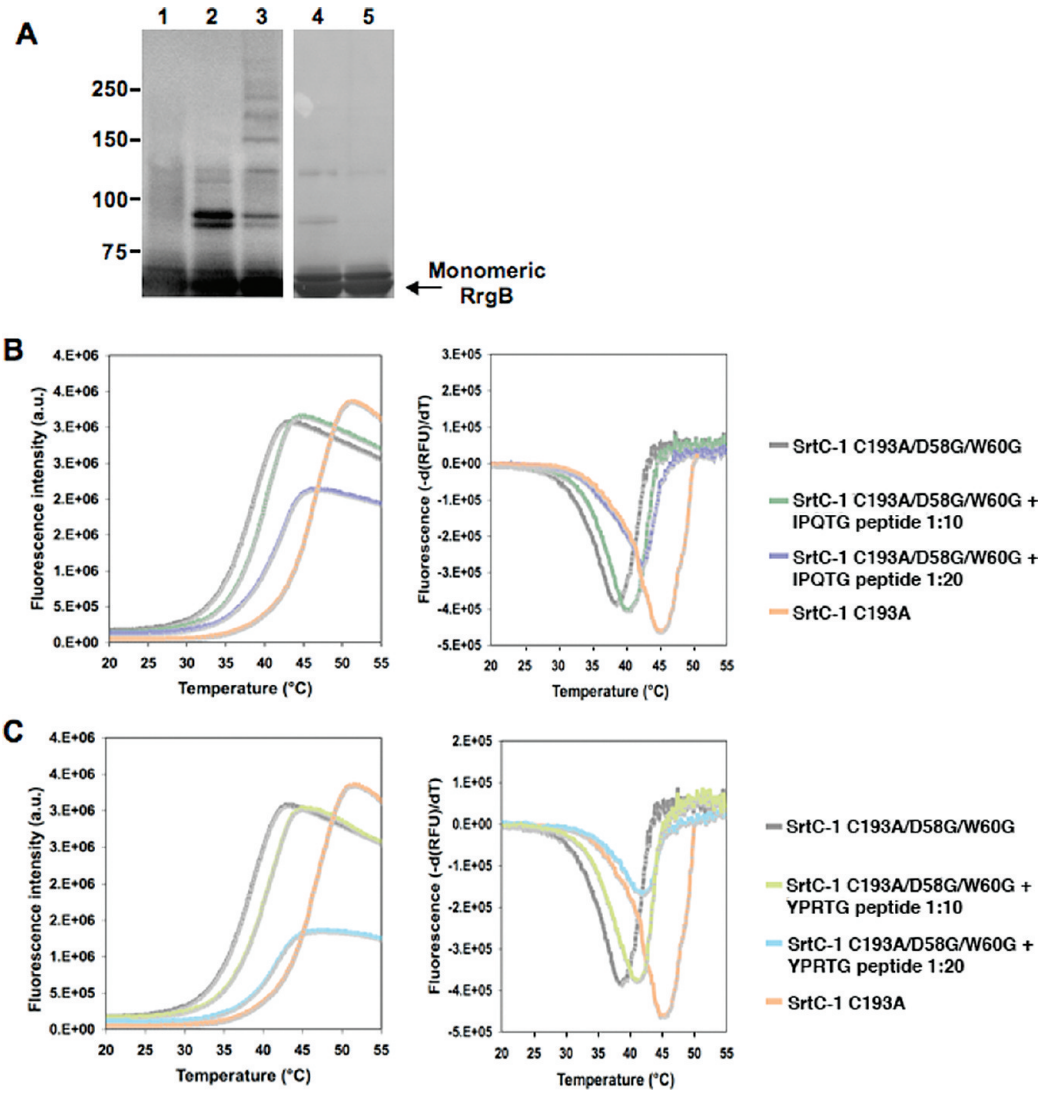

FIGURE 3: Activity and thermal stability studies of SrtC-1 carrying mutations in the lid anchor residues. (A) Western blot developed with antiserum against RrgB shows that SrtC-1 D58G/W60G polymerizes RrgB less efficiently. Lanes: (1) monomeric RrgB; (2) RrgB + SrtC-1 D58G/W60G; (3) RrgB + wild-type SrtC-1; (4) RrgB + SrtC-1 (lidC-2); (5) RrgB + SrtC-2 (lidC-1). The values on the left correspond to molecular mass marker sizes in kDa. The bands that run below the 100 kDa marker in lanes 2 and 4 correspond to an initial complex between RrgB and the SrtC-1 mutants which cannot be efficiently polymerized. (B) Thermal unfolding studies of SrtC-1 C193A/D58G/W60G in the presence of IPQTG, which corresponds to RrgB's LPXTG-like motif. The incubation of SrtC-1 C193A/D58G/W60G with the IPQTG peptide at two increasing protein:peptide molar ratios (1:10 and 1:20) suggests a stabilization of the mutant by the peptide. (C) Thermal unfolding studies of SrtC-1 C193A/D58G/W60G in the presence of YPRTG, which corresponds to RrgA's LPXTG-like motif. In both (B) and (C), the right panels represent the first derivative of the denaturation curves shown on the left.

identified in experiments performed with SrtC-1 D58G/W60G, which was shown (Figure 3A) to display some RrgB-polymerizing capabilities, but no evidence of the complex could be detected with mutants SrtC-1 C193A, SrtC-1 H131D, or SrtC-1 R202E (data not shown). These results indicate that the RrgB polymerization reaction proceeds through an acyl-complex intermediate whose formation is dependent on an intact catalytic triad and which can be trapped *in vitro*.

DISCUSSION

Pilus biosynthesis in Gram-positive bacteria requires the action of dedicated sortases in order to guarantee the covalent association of its building blocks (*36*). The pilus biosynthesis *rlrA* pathogenicity islet of *S. pneumoniae* encodes three sortase enzymes (SrtC-1, SrtC-2, SrtC-3) that do not display strict substrate specificities toward Rrg molecules, although SrtC-1 has been shown to be the key protein in formation of the RrgB fiber backbone (*11*, *31*). In this work, we have shown that, as is the case for nonpilus-related sortases, a triad composed of Cys, Arg, and His residues is essential for the catalytic activity of SrtC-1. Although the side chain of His131 is located more than 5 Å away from the nucleophilic Cys193 and its mutation into Asp does not affect protein stability, this modification completely blocks SrtC-1's fiber formation ability. Interestingly, mutation of Arg202 into Glu, in addition to generating a catalytically inactive SrtC-1, also affects enzyme stability, most probably due to the loss of two hydrogen bonds with an anchor lid residue (Asp58; see below).

We were also able to identify a "trapped" RrgB−SrtC-1 covalent intermediate in the reaction catalyzed by wild-type SrtC-1 by Western blotting and LC-MS/MS. Since sortase activity involves the formation of a covalent bond between the catalytic Cys and the Thr in the LPXTG motif of the substrate, it is conceivable that the intermediate identified here represents a

A

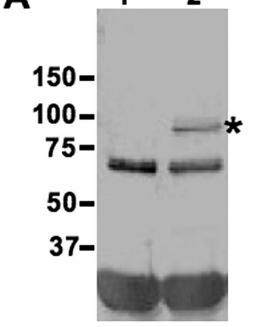

B

Experimental Molecular Mass (Da)	Calculated Molecular Mass (Da)	Corresponding protein species
23786	23782.9	*SrtC-1*
64933	65054.5	*RrgB*
88372	88837.4	*SrtC-1/RrgB complex*

C

Observed	Mr (expt)	Mr (calc)	Delta	First	Last	Sequence	Identified protein
911.57	1821.13	1820.91	0.21	210	225	IPYVAEVEEEFIAANK	*SrtC-1*
663.35	1324.70	1324.63	0.07	159	169	EVMAYQVDQVK	*SrtC-1*
508.28	1521.82	1521.69	0.13	30	42	ATLDEADIDERMK	*SrtC-1*
523.84	1045.67	1045.56	0.11	129	138	FNTANLPAAK	*RrgB*
563.35	1124.69	1124.57	0.12	300	309	ITYSATLNDK	*RrgB*
588.87	1175.72	1175.63	0.09	580	590	QPAGYALLTSR	*RrgB*
602.88	1203.75	1203.67	0.08	377	387	VVQTVTLTTDK	*RrgB*
740.43	1478.85	1478.72	0.12	431	443	DENPKPLDPTEPK	*RrgB*
566.01	1695.02	1694.85	0.17	388	402	NTVTVNGLDKNTEYK	*RrgB*
639.39	1915.14	1914.92	0.22	410	427	GYSADYQEITTAGEIAVK	*RrgB*
688.76	2063.25	2063.04	0.21	461	480	LAGAEFVIANADNAGQYLAR	*RrgB*
749.49	2245.45	2245.22	0.24	377	397	VVQTVTLTTDKNTVTVNGLDK	*RrgB*
781.14	2340.39	2340.15	0.24	141	162	IYEIHSLSTYVGEDGATLTGSK	*RrgB*
828.85	2483.54	2483.25	0.28	206	227	VDKDTPVNHQVGDVVEYEIVTK	*RrgB*
857.17	2568.49	2568.20	0.29	42	65	LLATDGDMDKIANELETGNYAGNK	*RrgB*

FIGURE 4: SrtC-1 and RrgB form a covalent complex. (A) Western blot developed with SrtC-1 antiserum. Lanes: (1) monomeric SrtC-1; (2) RrgB + SrtC-1. Monomeric SrtC-1 migrates as a band with an approximate molecular mass of 23 kDa; a small amount of dimeric SrtC-1, which migrates above its theoretical mass of 47.4 kDa, is also visible. The RrgB/SrtC-1 covalent complex is indicated with a star. (B) MALDI results of the mix between SrtC-1 and RrgB, which identifies not only the single proteins but also a mass of approximately 88 kDa, which corresponds to a covalent complex. On occasion, the SrtC-1 dimer could also be identified, yielding a mass value of 47573 Da. (C) LC-MS/MS results for the band indicated with a star in (A). The lanes correspond to the following: observed, mass to charge ratio (m/z) of peptide; M_r (expt), experimental molecular mass (Da) of peptide; M_r (calc), calculed molecular mass (Da) of peptide; Delta, mass difference (Da) between M_r (expt) and M_r (calc); First, identification of the first amino acid of the peptide in the full-length protein; Last, identification of the last amino acid of the peptide on the full-length protein; Sequence, sequence of the identified peptide.

form in which SrtC-1 and RrgB are covalently associated through Cys193 (SrtC-1) and Thr631 (RrgB). Notably, it is most likely that identification of the covalent form was only possible because, although the RrgB fiber can be formed *in vitro*, the SrtC-1 RrgB polymerization reaction under these conditions is slow and/or inefficient, allowing the intermediate to be identified. The covalent intermediate was also identified in experiments in which the SrtC-1 D58G/W60G mutant was incubated with RrgB (Figure 3A, lane 2); this indicates that mutation of the lid anchor residues does not block either substrate recognition or acyl-enzyme formation but affects reaction processivity. It is conceivable that, in the SrtC-1 D58G/W60G mutant, the flexible lid continues to provide pilin access to the active site, but polymerization is compromised due to enzyme instability. Notably, no bands for the covalent intermediate could be identified in SrtC-1 mutants in which the His131 or Arg202 side chains were mutated. The absence of fiber-formation activity and the inability of Arg and His active site mutants to form the acyl-enzyme complex suggest that both residues participate in a catalytic step prior to acyl-enzyme formation. In SrtA, the catalytic His residue has been hypothesized as being responsible for the protonation of the substrate leaving group, while the Arg side chain could stabilize the negative charge accumulation in the transition state (*22*, *26*, *37*) or participates in positioning of the substrate by direct interaction with backbone residues (*25*). Thus, acyl-enzyme trapping can be enhanced by mutation of either of the two auxiliary members of the catalytic triad, His or Arg. It is also of note that recently Guttilla and co-workers were able to trap pilus polymerization acyl-enzyme intermediates on the surface of *C. diphtheriae* mutants (*38*), revealing that the formation of a covalent complex in the pilus biogenesis process of Gram-positive species is also identifiable directly on the bacterial surface.

Sortases involved in pilus formation in a variety of bacterial species carry lid regions with two anchor residues (Figure 2B). In SrtC-1, these key residues (Asp58 and Trp60) anchor the lid in a seemingly closed conformation. Since, in the structure of SrtC-3, Trp60 is replaced by a Phe (*31*), it seems likely that the hydrophobic nature of this residue plays a role in lid closure. Asp58, however (which is invariably an Asp in all sequences of pilus-related sortases known to date; examples in Figure 2B), plays a key role in stabilizing Arg202 (thus, a member of the catalytic triad) through two hydrogen bonds, with the side chain facing the Cys nucleophile directly. Absence of the two lid anchor side chains not only starkly diminishes SrtC-1's capacity to polymerize RrgB fibers but also causes protein destabilization. This behavior is also observed in SrtC-1 and SrtC-2 mutant forms in which the respective lid regions were switched. Interestingly, protein stability can be partly recovered through the addition of the LPXTG-like peptides, which have been suggested to lodge within the elongated cleft upon lid opening. These results support the proposition that lid movement is required prior to/concomitant with substrate accommodation within the binding site (*31*). The observation that large amounts of the LPXTG-like peptides cannot totally recover SrtC-1 stability suggests that other features

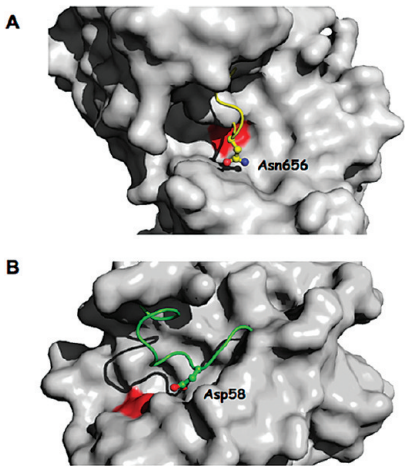

FIGURE 5: Access to transpeptidation active sites in PBPs and sortases is regulated by flexible lids. Surface representations of (A) PBP1b from *S. pneumoniae* and (B) SrtC-1, with active site residues represented in red. Both transpeptidases display lid regions (yellow for PBP1b, green for SrtC-1) which are maintained in closed conformation in the absence of ligand. Polar residues Asn656 (A) and Asp58 (B) play key roles in maintaining lids in a closed form.

of the full-length RrgB substrate also play a role in SrtC-1 recognition and stabilization.

The presence of a flexible lid that covers the active site in pilus-related sortases, studied here, is also detected in other transpeptidases. Suree and co-workers (*25*) have identified that the access of substrate to the active site of SrtA from *S. aureus*, an enzyme involved in the covalent association of virulence factors to the peptidoglycan, is also regulated by a flexible loop. Although this region corresponds to a loop which is in a different position from the lid described in this work for sortases involved in pilus formation (Figure 2B), it points to the possibility that sortases control access of substrate to their active site through the movement of surrounding flexible regions. Interestingly, another class of well-studied transpeptidases, penicilin-binding proteins (PBPs), also carry a malleable region in close proximity to the active site (located between β3 and β4 (*39*−*45*)). The transpeptidase domains of PBPs catalyze the cross-linking of stem peptides of the peptidoglycan, thus recognizing peptidic substrates within the cleft, much like sortases; in addition, they are the targets for β-lactam antibiotics, whose structure mimics the last two residues of the stem peptide (*46*). Thus, it is of interest that, in the crystal structure of PBP1b from *S. pneumoniae*, the β3/β4 loop maintains the active site in "closed" conformation in the absence of ligand largely through its obstruction by a polar residue (Asn656) (*41*). Notably, opening of the cleft can only be achieved *in vitro* through incubation with substrate or a pseudosubstrate which structurally mimics the pentapeptide. This incubation, which causes an "opening" movement of the loop, allows trapping of an acyl-enzyme intermediate as well as complex formation with different β-lactam and γ-lactam antibiotics, suggesting that substrate/pseudosubstrate recognition and lid opening are related events (*47*, *48*). Thus, due to the similarity in substrate recognition patterns and catalytic functionality, a common mechanism of regulation of active site access could be proposed for both sortase and PBP transpeptidases. In the absence of substrate (stem peptides for PBPs, LPXTG-like peptides for sortases) the catalytic cleft is maintained in closed conformation through specific interactions generated by lid residues (Figure 5). However, once substrate becomes available (i.e., when peptidoglycan biosynthesis is required during different moments of the cell cycle (PBPs) or when virulence factor subunits must be attached to partner molecules (sortases)), the lid is opened, potentially through direct interaction with substrates. These observations lend support to the idea that conformational changes induced by ligand binding should be taken into consideration in transpeptidase-targeted drug design efforts.

ACKNOWLEDGMENT

The authors thank Carlos Contreras-Martel (IBS) for help during the initial phases of the project, the ESRF ID29 beamline staff for help with data collection, Izabel Bérard and Eric Forest from the IBS mass spectroscopy facility (LSMP, IBS) for analyses, Alexandra Kraut and Jérôme Garin (Laboratoire d'Etude de la Dynamique des Protéomes, EDyP Grenoble) for access to the LC-MS/MS platform and experiments, and the RoBioMol facility (IBS) for access to the TSA equipment.

REFERENCES

1. Telford, J. L., Barocchi, M. A., Margarit, I., Rappuoli, R., and Grandi, G. (2006) Pili in Gram-positive pathogens. *Nat. Rev. Microbiol. 4*, 509–519.
2. Proft, T., and Baker, E. N. (2009) Pili in Gram-negative and Gram-positive bacteria—structure, assembly, and their role in disease. *Cell. Mol. Life Sci. 66*, 613–635.
3. Sauer, F. G., Pinkner, J. S., Waksman, G., and Hultgren, S. J. (2002) Chaperone priming of pilus subunits facilitates a topological transition that drives fiber formation. *Cell 111*, 543–551.
4. Vetsch, M., Puorger, C., Spirig, T., Grauschopf, U., Weber-Ban, E. U., and Glockshuber, R. (2004) Pilus chaperones represent a new type of protein-folding catalyst. *Nature 431*, 329–332.
5. LeMieux, J., Hava, D. L., Basset, A., and Camilli, A. (2006) RrgA and RrgB are components of a multisubunit pilus encoded by the *Streptococcus pneumoniae* rlrA pathogenicity islet. *Infect. Immun. 74*, 2453–2456.
6. Mora, M., Bensi, G., Capo, S., Falugi, F., Zingaretti, C., Manetti, A. G. O., Maggi, T., Taddei, A. R., Grandi, G., and Telford, J. L. (2005) Group A *Streptococcus* produce pilus-like structures containing protective antigens and Lancefield T antigens. *Proc. Natl. Acad. Sci. U.S.A. 102*, 15641–15646.
7. Ton-That, H., Marraffini, L. A., and Schneewind, O. (2004) Sortases and pilin elements involved in pilus assembly of *Corynebacterium diphtheriae*. *Mol. Microbiol. 53*, 251–261.
8. Barocchi, M. A., Ries, J., Zogaj, X., Hemsley, C., Albiger, B., Kanth, A., Dahlberg, S., Fernebro, J., Moschioni, M., Masignani, V., Hultenby, K., Taddei, A. R., Beiter, K., Wartha, F., von Euler, A., Covacci, A., Holden, D. W., Normark, S., Rappuoli, R., and Henriques-Normark, B. (2006) A pneumococcal pilus influences virulence and host inflammatory responses. *Proc. Natl. Acad. Sci. U.S.A. 103*, 2857–2862.
9. Hilleringmann, M., Giusti, F., Baudner, B. C., Masignani, V., Covacci, A., Rappuoli, R., Barocchi, M. A., and Ferlenghi, I. (2008) Pneumococcal pili are composed of protofilaments exposing adhesive clusters of RrgA. *PLoS Pathogens 4*, e1000026.
10. Nelson, A. L., Ries, J., Bagnoli, F., Dahlberg, S., Falkner, S., Rounioja, S., Tschop, J., Morfeldt, E., Ferlenghi, I., Hilleringmann, M., Holden, D. W., Rappuoli, R., Normark, S., Barocchi, M. A., and Henriques-Normark, B. (2007) RrgA is a pilus-associated adhesin in *Streptococcus pneumoniae*. *Mol. Microbiol. 66*, 329–340.
11. Fälker, S., Nelson, A. L., Morfeldt, E., Jonas, K., Hultenby, K., Ries, J., Melefors, O., Normark, S., and Henriques-Normark, B. (2008) Sortase-mediated assembly and surface topology of adhesive pneumococcal pili. *Mol. Microbiol. 70*, 597–607.
12. LeMieux, J., Woody, S., and Camilli, A. (2008) The roles of the sortases of *Streptococcus pneumoniae* in assembly of the RlrA pilus. *J. Bacteriol.* (e-print).
13. Dramsi, S., Magnet, S., Davison, S., and Arthur, M. (2008) Covalent attachment of proteins to peptidoglycan. *FEMS Microbiol. Rev. 32*, 307–320.
14. Neiers, F., Madhurantakam, C., Fälker, S., Manzano, C., Dessen, A., Normark, S., Henriques-Normark, B., and Achour, A. (2009) Two crystal structures of pneumococcal pilus sortase C provide novel insights into catalysis and substrate specificity. *J. Mol. Biol.* (eprint).

15. Marraffini, L. A., DeDent, A. C., and Schneewind, O. (2006) Sortases and the art of anchoring proteins to the envelopes of Gram-positive bacteria. *Microb. Mol. Biol. Rev. 70*, 192–221.
16. Mazmanian, S. K., Skaar, E. P., Gaspar, A. H., Humayun, M., Gornicki, P., Jelenska, J., Joachimiak, A., Missiakas, D. M., and Schneewind, O. (2003) Passage of heme-iron across the envelope of *Staphylococcus aureus*. *Science 299*, 906–909.
17. Schneewind, O., Model, P., and Fischetti, V. A. (1992) Sorting of protein A to the staphylococcal cell wall. *Cell 70*, 267–281.
18. Ton-That, H., Mazmanian, S. K., Alksne, L., and Schneewind, O. (2002) Anchoring of surface proteins to the cell wall of *Staphylococcus aureus*. *J. Biol. Chem. 277*, 7447–7452.
19. Mandlik, A., Swierczynski, A., Das, A., and Ton-That, H. (2008) Pili in Gram-positive bacteria: assembly, involvement in colonization and biofilm development. *Trends Microbiol. 16*, 33–40.
20. Zhang, R., Wu, R., Joachimiak, G., Mazmanian, S. K., Missiakas, D. M., Gornicki, P., Schneewind, O., and Joachimiak, A. (2004) Structures of sortase B from *Staphylococcus aureus* and *Bacillus anthracis* reveal catalytic amino acid triad in the active site. *Structure 12*, 1147–1156.
21. Ilangovan, U., Ton-That, H., Iwajara, J., Schneewind, O., and Clubb, R. T. (2001) Structure of sortase, the transpeptidase that anchors proteins to the cell wall of *Staphylococcus aureus*. *Proc. Natl. Acad. Sci. U.S.A. 98*, 6056–6061.
22. Maresso, A. W., Wu, R., Kern, J. W., Zhang, R., Janik, D., Missiakas, D. M., Duban, M.-E., Oachimiak, A., and Schneewind, O. (2007) Activation of inhibitors by sortase triggers irreversible modification of the active site. *J. Biol. Chem. 282*, 23129–23139.
23. Zong, Y., Mazmanian, S. K., Schneewind, O., and Narayana, S. V. L. (2004) The structure of sortase B, a cysteine transpeptidase that tethers surface protein to the *Staphylococcus aureus* cell wall. *Structure 12*, 105–112.
24. Zong, Y., Bice, T. W., Ton-That, H., Schneewind, O., and Narayana, S. V. L. (2004) Crystal structure of *Staphylococcus aureus* sortase A and its substrate complex. *J. Biol. Chem. 279*, 31383–31389.
25. Suree, N., Liew, C. K., Villareal, V. A., Thieu, W., Fadeev, E. A., Clemens, J. J., Jung, M. E., and Clubb, R. T. (2009) The structure of the *Staphylococcus aureus* sortase-substrate complex reveals how the universally conserved LPXTG sorting signal is recognized. *J. Biol. Chem. 284*, 24465−24477.
26. Frankel, B. A., Tong, Y., Bentley, M. L., Fitzgerald, M. C., and McCafferty, D. G. (2007) Mutational analysis of active site residues in the *Staphylococcus aureus* transpeptidase SrtA. *Biochemistry 46*, 7269–7278.
27. Marraffini, L. A., Ton-That, H., Zong, Y., Narayana, S. V. L., and Schneewind, O. (2004) Anchoring of surface proteins to the cell wall of *Staphylococcus aureus*: a conserved arginine residue is required for efficient catalysis of sortase A. *J. Biol. Chem. 279*, 37763–37770.
28. Liew, C. K., Smith, B. T., Pilpa, R., Suree, N., Ilangovan, U., Connolly, K. M., Jung, M. E., and Clubb, R. T. (2004) Localization and mutagenesis of the sorting signal binding site on sortase A from *Staphylococcus aureus*. *FEBS Lett. 571*, 221–226.
29. Scott, J. R., and Zahner, D. (2006) Pili with strong attachments: Gram-positive bacteria do it differently. *Mol. Microbiol. 62*, 320–330.
30. Hava, D. L., and Camilli, A. (2002) Large-scale identification of serotype 4 *Streptococcus pneumoniae* virulence factors. *Mol. Microbiol. 45*, 1389–1405.
31. Manzano, C., Contreras-Martel, C., El Mortaji, L., Izore, T., Fenel, D., Vernet, T., Schoehn, G., Di Guilmi, A. M., and Dessen, A. (2008) Sortase-mediated pilus fiber biogenesis in *Streptococcus pneumoniae*. *Structure 16*, 1838–1848.
32. Kabsch, W. (1993) Automatic processing of rotation diffraction data from crystals of initially unknown symmetry and cell constants. *J. Appl. Crystallogr. 26*, 795–800.
33. Storoni, L., McCoy, A., and Read, R. (2004) Likelihood-enhanced fast rotation functions. *Acta Crystallogr., Sect. D 57*, 1373–1382.
34. Murshudov, G., Vagin, A., and Dodson, E. (1997) Refinement of macromolecular structures by the maximum-likelihood method. *Acta Crystallogr., Sect. D 53*, 240–255.
35. Emsley, P., and Cowtan, K. (2004) Coot: model-building tools for molecular graphics. *Acta Crystallogr., Sect. D 60*, 2126–2132.
36. Ton-That, H., and Schneewind, O. (2004) Assembly of pili in Gram-positive bacteria. *Trends Microbiol. 12*, 228–234.
37. Frankel, B. A., Kruger, R. G., Robinson, D. A., Kelleher, N. L., and McCafferty, D. G. (2005) *Staphylococcus aureus* sortase transpeptidase SrtA: insight into the kinetic mechanism and evidence for a reverse protonation catalytic mechanism. *Biochemistry 44*, 11188–11200.
38. Guttilla, I. K., Gaspar, A. H., Swierczynski, A., Swaminathan, A., Dwivedi, P., Das, A., and Ton-That, H. (2009) Acyl enzyme intermediates in the sortase-catalyzed pilus morphogenesis in Gram-positive bacteria. *J. Bacteriol. 191*, 5603−5612.
39. Contreras-Martel, C., Dahout-Gonzalez, C., Dos Santos Martins, A., Kotnik, M., and Dessen, A. (2009) PBP active site flexibility as the key mechanism for beta-lactam resistance in pneumococci. *J. Mol. Biol. 387*, 899–909.
40. Lim, D., and Strynadka, N. C. (2002) Structural basis for the beta lactam resistance of PBP2a from methicillin-resistant *Staphylococcus aureus*. *Nat. Struct. Biol. 9*, 870–876.
41. Macheboeuf, P., Di Guilmi, A. M., Job, V., Vernet, T., Dideberg, O., and Dessen, A. (2005) Active site restructuring regulates ligand recognition in class A penicillin-binding proteins. *Proc. Natl. Acad. Sci. U.S.A. 102*, 577–582.
42. Pernot, L., Chesnel, L., Le Gouellec, A., Croize, J., Vernet, T., Dideberg, O., and Dessen, A. (2004) A PBP2x from a clinical isolate of *Streptococcus pneumoniae* exhibits an alternative mechanism for reduction of susceptibility to β-lactam antibiotics. *J. Biol. Chem. 279*, 16463–16470.
43. Powell, A. J., Tomberg, J., Deacon, A. M., Nicholas, R. A., and Davies, C. (2008) Crystal structures of penicillin-binding protein 2 from penicillin-susceptible and -resistant strains of *N. gonorrhoeae* reveal an unexpectedly subtle mechanism for antibiotic resistance. *J. Biol. Chem. 284*, 1202–1212.
44. Sauvage, E., Kerff, F., Fonze, E., Herman, R., Schoot, B., Marquette, J. P., Taburet, Y., Prevost, D., Dumas, J., Leonard, G., Stefanic, P., Coyette, J., and Charlier, P. (2002) The 2.4 Å crystal structure of the penicillin-resistant penicillin-binding protein PBP5fm from *Enterococcus faecium* in complex with benzylpenicillin. *Cell. Mol. Life Sci. 59*, 1223–1232.
45. Job, V., Carapito, R., Vernet, T., Dessen, A., and Zapun, A. (2008) Common alterations in PBP1a from resistant *Streptococcus pneumoniae* decrease its reactivity towards beta-lactams: structural insights. *J. Biol. Chem. 283*, 4886–4894.
46. Höltje, J. V. (1998) Growth of the stress-bearing and shape-maintaining murein sacculus of *Escherichia coli*. *Microbiol. Mol. Biol. Rev. 62*, 181–203.
47. Macheboeuf, P., Lemaire, D., Thaller, N., Dos Santos Martins, A., Luxen, A., Dideberg, O., Jamin, M., and Dessen, A. (2007) Trapping of an acyl-enzyme intermediate in a penicillin-binding protein (PBP) catalyzed reaction. *J. Mol. Biol. 376*, 405–413.
48. Macheboeuf, P., Fischer, D. S., Brown, T., Jr., Zervosen, A., Luxen, A., Joris, B., Dessen, A., and Schofield, C. J. (2007) Structural and mechanistic basis of penicillin-binding protein inhibition by lactivicins. *Nat. Chem. Biol. 3*, 565–569.